Acta of Bioengineering and Biomechanics
Vol. 26, No. 3, 2024

Original paper
DOI: 10.37190/ABB-02504-2024-02

Comparison of stop-jump muscle synergies in amateur basketball players with and without asymptomatic patellar tendon abnormalities during simulated games

DONGXU WANG[1], DONG SUN[1], ZHANYI ZHOU[1], FENGPING LI[1], XUANZHEN CEN[1], YANG SONG[2], MONÈM JEMNI[3], YAODONG GU[1]*

[1] Faculty of Sports Science, Ningbo University, Ningbo, China.
[2] Department of Biomedical Engineering, Faculty of Engineering, The Hong Kong Polytechnic University, Hong Kong, China.
[3] Centre for Mental Health Research in Association, University of Cambridge, Cambridge, UK.

Purpose: Asymptomatic patellar tendon abnormality (APTA) is considered a precursor to patellar tendinopathy (PT), but its pathogenesis remains unclear, especially regarding changes in muscle coordination. Therefore, it is essential to explore the muscle synergy patterns in individuals with APTA. *Methods*: This study recorded sEMG data during stop-jump tasks in 8 APTA and 8 healthy amateur male basketball players in a simulated basketball game. Muscle synergies were extracted using Non-Negative Matrix Factorization and *K*-Means clustering. *Results*: Three synergies were identified in both groups. In Synergy 1, tibialis anterior, semitendinosus and vastus lateralis weights primarily influenced the waveform. In Synergy 2, biceps femoris, vastus lateralis and medial gastrocnemius weights primarily influenced the waveform. In Synergy 3, peroneus longus, vastus medialis and vastus lateralis weights primarily influenced the waveform. Key findings include higher vastus medialis weight in the APTA group during P1 and P2, and higher semitendinosus weight in P3 and P4. Additionally, the gastrocnemius and biceps femoris showed significant differences between groups across phases. *Conclusions*: The APTA group exhibited different muscle synergy patterns under specific phases and load accumulation conditions, particularly in the vastus medialis, medial gastrocnemius, biceps femoris and peroneus longus. The APTA group demonstrated distinct synergy patterns, suggesting a compensatory mechanism to reduce patellar tendon load, potentially increasing knee injury risk. This finding provides new guidance for clinical assessment and intervention strategies for the training and rehabilitation of APTA individuals.

Key words: *asymptomatic patellar tendon abnormalities, basketball exercise simulation, motor control, K-means clustering, non-negative matrix factorization*

1. Introduction

Patellar tendinopathy (PT) is a common overuse injury of the knee, frequently occurring in sports involving repetitive jumping and landing. A multidisciplinary sports club study conducted over eight seasons found that the incidence of PT among professional basketball players was 22.7%, with guards exhibiting the highest incidence due to the frequent jumping involved in their position [36]. Given the high incidence of PT and its severe impact on athletes' careers, understanding the injury mechanisms of patellar tendinopathy and developing effective prevention strategies are particularly important.

The clinical diagnosis of PT is based on the patient's symptoms (such as patellar tendon pain), while ultrasound imaging is considered the standard tool for diagnosing patellar tendon abnormality (PTA). On ultrasound images, PTA typically appears as a hypoechoic region. Previous studies have shown that PTA can be found even in asymptomatic athletes, and this abnor-

* Corresponding author: Yaodong Gu, Faculty of Sports Science, Ningbo University, Ningbo, China. E-mail: guyaodong@nbu.edu.cn
Received: September 3rd, 2024
Accepted for publication: October 3rd, 2024

mality is often considered a precursor to PT [19]. Without timely rehabilitation treatment, PTA may gradually develop into PT, with an occurrence probability of 22–32% [35]. Although previous studies have compared patellar tendinopathy patients with healthy individuals, the mechanisms by which PTA evolves into patellar tendinopathy remain unclear [11], [21]. Therefore, this study conducted a prospective study on individuals with asymptomatic patellar tendon abnormality (APTA), to explore its relationship with the development of patellar tendinopathy.

Studies have found that basketball players with PTA tend to reduce the load on the patellar tendon during stop-jump maneuvers through compensatory mechanisms, such as increased hip flexion [30]. Edwards et al. [10] discovered that during the horizontal landing phase, PTA patients typically activate the semitendinosus (ST) and biceps femoris (BF) first, while healthy individuals are more likely to first activate the tibialis anterior (TA) and medial gastrocnemius (MG). These findings suggest that PTA patients adjust their motor control strategies during stop-jump tasks to accommodate their biomechanical changes or achieve better athletic performance [15]. Although previous studies have investigated the neuromuscular control strategies of athletes after knee injuries, there is still a lack of systematic research on the specific changes in muscle synergy patterns in individuals with asymptomatic patellar tendon abnormality (APTA) during high-load movement tasks [6]. At the same time, biomechanical characteristics are actually the result of the nervous system interacting with the external environment under task constraints and biomechanical limitations of the limbs [25]. Therefore, analyzing only kinematic, kinetic or individual muscle electrical activity characteristics provides limited understanding of the specific impact of PTA on motor control strategies [10]. Given the complex synergy among most muscles [22], accurately identifying neuromuscular control strategies in specific tasks and gaining comprehensive insights necessitates considering the synergistic interaction of multiple muscles in an integrated manner. Therefore, it is important to study the specific changes in muscle synergy patterns in the APTA population.

In recent years, scientists have employed a technique called Non-Negative Matrix Factorization (NMF) to study the coordination of muscles during movement [26]. NMF analysis helps identify the collaborative relationships between muscles and their activation timing. In simple terms, muscle synergies function like a team, where different muscles work together to perform specific actions, and the activation coefficients indicate when this team is mobilized [26]. Because NMF is based on the non-negativity of matrix factors, it offers greater interpretability of results, while also being easy to implement and having low memory requirements [42]. Recently, NMF has gradually expanded into the field of sports science and has shown potential in enhancing athletic performance and preventing sports injuries [8], [20].

Based on the aforementioned research background, this study aims to explore the impact of specialized loading on neuromuscular control strategies during stop--jump tasks from the perspective of muscle synergies. It seeks to clarify the significance of muscle synergies during different phases of the stop-jump task and analyze the synergy differences between APTA and healthy individuals across different dimensions (time-space). Understanding these differences is crucial for elucidating the pathogenesis of patellar tendinopathy and developing prevention strategies. We hypothesize that there will be no difference in the number of muscle synergies between the two groups, but that the APTA group, compared to the healthy group, will exhibit different motor modules by adjusting muscle activation weights to adapt to biomechanical changes induced by their condition.

2. Materials and methods

2.1. Subjects

A total of 8 asymptomatic PTA and 8 healthy amateur male basketball players were recruited for this study, with detailed participant information provided in Table 1. Inclusion criteria included: no history of professional basketball training, self-training 1–2 times per week [27]. All participants were right-leg dominant and had no history of traumatic lower limb injury in the past 6 months [37]. Patellar tendon morphology was assessed by an experienced musculoskeletal ultrasound physician using a 13 MHz linear array portable ultrasound device (Siemens Antares, Siemens AG, Germany), with ultrasound abnormalities recorded. Ultrasound abnormalities were defined as hypoechoic areas ≥2 mm [4]. Finally, 8 athletes showing patellar tendon abnormalities on ultrasound were assigned to the asymptomatic patellar tendon abnormality (APTA) group, and 8 matched healthy athletes were assigned to the control group. All participants signed a written informed consent form before data collection. The study protocol was approved by the Scientific Research Ethics Committee of Ningbo University (Approval Number: RAGH20231120).

Table 1. Information of the eligible participants

Variable	APTA (n = 8)	Healthy (n = 8)	p
	Mean (SD)	Mean (SD)	
Age [years]	23.0 (3.5)	22.8 (4.0)	0.693
Height [m]	1.80 (0.6)	1.82 (0.7)	0.602
Weight [kg]	75.0 (8.5)	77.1 (8.1)	0.557
BMI [kg/m^2]	23.9 (3.1)	23.5 (3.0)	0.654
Basketball experience [years]	5.5 (3.1)	5.1 (2.5)	0.434
Position of play	Point Guard	Point Guard	/

SD – standard deviation, APTA – Asymptomatic Patellar Tendon Abnormality.

2.2. Procedures

2.2.1. Experiments

The Basketball Exercise Simulation Test (BEST) consists of four 10-minute phases, strictly following official game time. Each BEST cycle includes 30 seconds of intermittent specific exercises, incorporating activities such as sprinting, jumping, running, jogging, sliding and recovery [34]. In Figure 1C, the various activities and distances involved in each BEST cycle are shown. Each cycle is limited to 30 seconds, requiring participants to perform continuously within each 10-minute interval (up to 20 cycles). Typically, participants complete a cycle within 25 seconds, allowing at least 5 seconds of rest to prepare for the next cycle. If participants fail to complete a cycle within the allotted time, they must stop immediately and begin the next cycle. The overall experimental procedure is shown in Fig. 1D.

Before the experiment, participants underwent a 5-minute standardized dynamic warm-up, including full-body dynamic and static stretching. In the main task of the experiment, participants took a step forward from a self-selected distance, firmly planting each foot on the ground, and then performed a vertical jump, attempting to touch a ball on the ceiling with their dominant

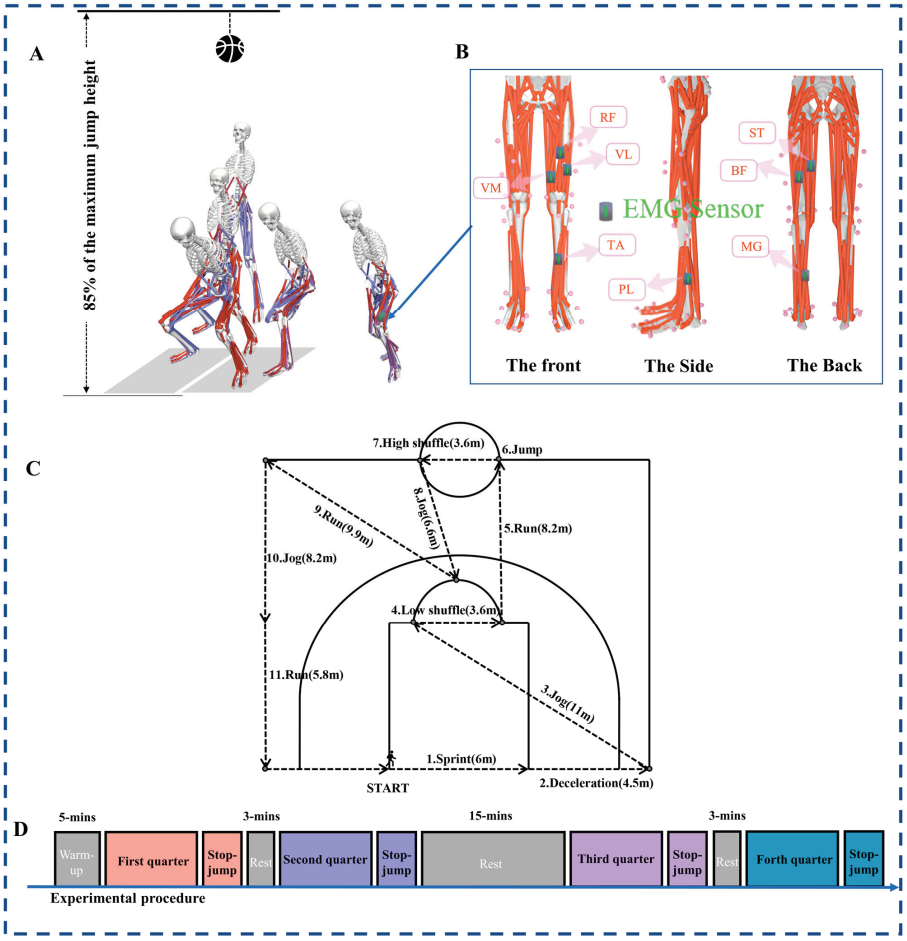

Fig. 1. Experimental protocol. (A) The process of the stop-jump movement, (B) EMG marker location, (C) A schematic depiction of the Basketball Exercise Simulation Test (BEST), (C) The overall experimental process. BF – biceps femoris, MG – medial gastrocnemius, PL – peroneus longus, RF – rectus femoris, ST – semitendinosus, TA – tibialis anterior, VL – vastus lateralis, VM – vastus medialis, High – high-intensity, Low – low-intensity

hand (Fig. 1A). Prior to the experiment, professional basketball players demonstrated and explained the tasks to ensure that all participants were familiar with the procedure and to ensure consistency in data collection. The criteria for successfully completing the stop-jump task were: (1) both feet must fully contact the ground; (2) participants must touch the ball on the ceiling. Participants were required to perform five stop-jumps, with the middle three trials used for further analysis. During the experiment, all subjects wore their own sports shoes [15], [40].

2.2.2. Data recording and preprocessing

According to the SENIAM guidelines for sEMG sensor placement and anatomical knowledge, the corresponding muscle locations were determined through a series of specific movements. The optimal positions on the muscle bellies were selected by an experienced researcher to ensure that the sensors were placed away from tendons or the edges of muscles [17]. Before electrode placement, excess hair was removed using a disposable razor, and the skin surface was carefully cleaned with 75% medical alcohol to remove oil and debris. The skin was allowed to dry to minimize skin impedance before attaching the electrodes. Using the EMGworks system (Delsys, Boston, USA), eight sEMG sensors were placed on the muscle bellies at predetermined locations: biceps femoris (BF) (50% of the distance between the ischial tuberosity and the lateral epicondyle of the tibia), medial gastrocnemius (MG) (at the most prominent bulge of the muscle), peroneus longus (PL) (at 25% of the line between the head of the fibula and the lateral malleolus), rectus femoris (RF) (50% of the line between the anterior superior iliac spine and the upper part of the patella), semitendinosus (ST) (50% of the distance between the ischial tuberosity and the medial epicondyle of the tibia), tibialis anterior (TA) (on the upper third of the line between the lateral condyle of the tibia and the medial malleolus), vastus lateralis (VL) (on the upper two-thirds of the line from the anterior superior iliac spine to the lateral side of the patella), and vastus medialis (VM) (at 80% of the line between the anterior superior iliac spine and the medial joint space of the knee). The sampling frequency was set to 1000 Hz, and all sEMG electrodes were aligned parallel to the direction of the muscle fibers, with an inter-electrode distance of 10 mm. Only data from the left limb were analyzed in this study, as the non-dominant leg is more frequently used for jumping and landing during layups in basketball [2], [19].

The preprocessing of sEMG signals was implemented using Matlab R2023b programming. First, the baseline of the raw sEMG data was zeroed. Then, a 4th--order Butterworth band-pass filter with a high-pass cutoff frequency of 30 Hz was applied to the raw sEMG signal to remove motion artifacts. Afterward, the signal was downsampled and full-wave rectified, followed by applying a 4th-order Butterworth low-pass filter with a cutoff frequency of 20 Hz to the rectified signal to extract the linear envelope [32]. Finally, all sEMG envelopes were interpolated to match the sampling point length of the same movement cycle and normalized to the maximum amplitude of the envelope during the stop-jump action [28].

2.2.3. Non-negative matrix factorization extracts muscle synergies

This study employed a Non-Negative Matrix Factorization (NMF) framework to extract muscle synergy components from sEMG data through linear decomposition based on unsupervised machine learning, with computations performed on the Rv4.4.1 platform. NMF decomposed the preprocessed sEMG signal matrix $V_{m\times n}$ into two non-negative matrices, as shown in Eq. (1).

$$V_{m\times n} = [\mathrm{EMG}_1\ \mathrm{EMG}_2\ \ldots\ \mathrm{EMG}_m]^T \approx \sum_{i=1}^{p} W_{m\times p} H_{p\times w} + e = V'_{m\times n}. \tag{1}$$

In this equation, V represents the original sEMG matrix, where m denotes the number of sEMG channels, and n denotes the number of samples. P is the number of muscle synergies obtained through NMF, where $m \geq p \geq 1$. $W_{m\times p}$ represents the muscle synergy vectors, and $H_{p\times w}$ represents the time activation coefficients. The reconstructed matrix $V'_{m\times n}$ is obtained by multiplying the W and H matrices and then adding the residual term e.

During the extraction of the basis and coefficient matrices using the Gaussian NMF Multiplicative Update Rules, the iteration stops when the R^2 change is less than 0.01% for 20 consecutive iterations, reaching the convergence threshold [32]. The quality of the NMF reconstruction is evaluated by the variance accounted for (VAF) to determine the optimal number of synergies. The steps for calculating VAF are as follows:

$$\mathrm{VAF} = \left(1 - \frac{\mathrm{RSS}}{\mathrm{TSS}}\right) \times 100\% = \left(1 - \frac{\Sigma (V - V')^2}{\Sigma (V - \bar{V})^2}\right) \times 100\%, \tag{2}$$

Table 2. The relationship between the number of synergies and VAF: The number of synergies is determined when VAF first exceeds 0.9

	Group	P1	P2	P3	P4	*p*
		Mean (SD)	Mean (SD)	Mean (SD)	Mean (SD)	
Num of Syn	APTA	3.02(0.02)	3.10(0.05)	3.11(0.05)	3.10(0.1)	0.522
	Healthy	3.20(0.07)	3.10(0.07)	3.05(0.01)	3.19(0.12)	0.310
	p	0.179	0.677	0.535	0.257	
VAF [%]						
2 Syn	APTA	78.23(5.12)	82.43(4.86)	85.66(5.19)	90.33(5.55)	0.097
	Healthy	81.46(4.71)	81.67(4.19)	80.57(5.59)	86.31(4.35)	0.355
	p	0.132	0.443	0.175	0.223	
3 Syn	APTA	90.23(3.15)	92.15(4.01)	95.01(2.23)	95.21(2.21)	0.294
	Healthy	93.11(2.31)	93.55(2.32)	91.13(4.33)	92.56(3.44)	0.501
	p	0.367	0.621	0.211	0.387	
4 Syn	APTA	93.00(2.01)	95.04(2.09)	94.09(1.44)	95.21(1.12)	0.621
	Healthy	94.01(2.00)	95.11(1.86)	94.22(1.03)	95.00(1.02)	0.533
	p	0.667	0.659	0.721	0.763	

P1 – phase 1, P2 – phase 2, P3 – phase 3, P4 – phase 4, SD – standard deviation, Num of Syn – the number of muscle synergies, VAF – variability accounted for, APTA – Asymptomatic Patellar Tendon Abnormality.

where: RSS refers to the residual sum of squares, and TSS refers to the total sum of squares. V represents the original muscle activation matrix. V' represents the NMF-reconstructed data matrix. $\overline{V}$ represents the mean of the original matrix V. To determine the optimal number of synergy components, this study calculated the VAF for the 1st to 6th order NMF decomposition results, and this was used to evaluate the optimal order, as shown in Table 2.

VAF > 90% is commonly used in the literature to identify the optimal number of synergies [31]. This criterion is considered to sufficiently represent the data, although its application remains debated [1]. For ease of comparison between groups, we selected the same number of muscle synergies as the rounded average of the synergies across all participants for further analysis [43]. The K-Means algorithm was used to cluster the muscle synergies of the APTA and Healthy groups separately, obtaining the overall synergy characteristics of athletes in different groups.

2.2.4. Statistical analysis

Muscle synergy data were processed using SPSS 23 statistical software, with results presented as means and standard deviations. To compare the differences in weight contributions of different muscles in each synergy, we conducted a two-way repeated measures ANOVA for each synergy. The two factors analyzed were group (APTA group and Healthy group) and load phase (P1, P2, P3, P4). When significant main effects or interaction effects were found, *post hoc* Bonferroni tests were used to further reveal specific differences. For violations of the sphericity assumption, we made adjustments using the Greenhouse–Geisser correction. Effect sizes were calculated using partial eta squared (η^2) to assess the magnitude of differences: <0.06 for small effects, 0.07–0.14 for medium effects and >0.14 for large effects.

3. Results

3.1. Choosing the optimal number of synergies under NMF

Muscle synergies can reflect the neuromuscular control strategies employed by athletes when performing movements [33]. In Figure 2, the VAF of muscle synergies in the APTA and Healthy groups across the four phases are shown. The interaction between groups and load accumulation on VAF was not statistically significant, $F(3, 21) = 0.661$, $p = 0.541$, $\eta^2 = 0.02$. In Table 2, it was shown that the number of muscle synergies in the APTA and Healthy groups at each phase were 3.02, 3.10, 3.11, and 3.10, and 3.20, 3.10, 3.05, and 3.19, respectively. To further compare the muscle synergy structures between groups, we rounded the number of synergies to 3. The results showed that when 3 muscle synergies were extracted, the VAFs for the APTA and Healthy groups at the four phases were 90.23, 92.15, 95.01, 95.21, 93.11, 93.55, 91.13 and

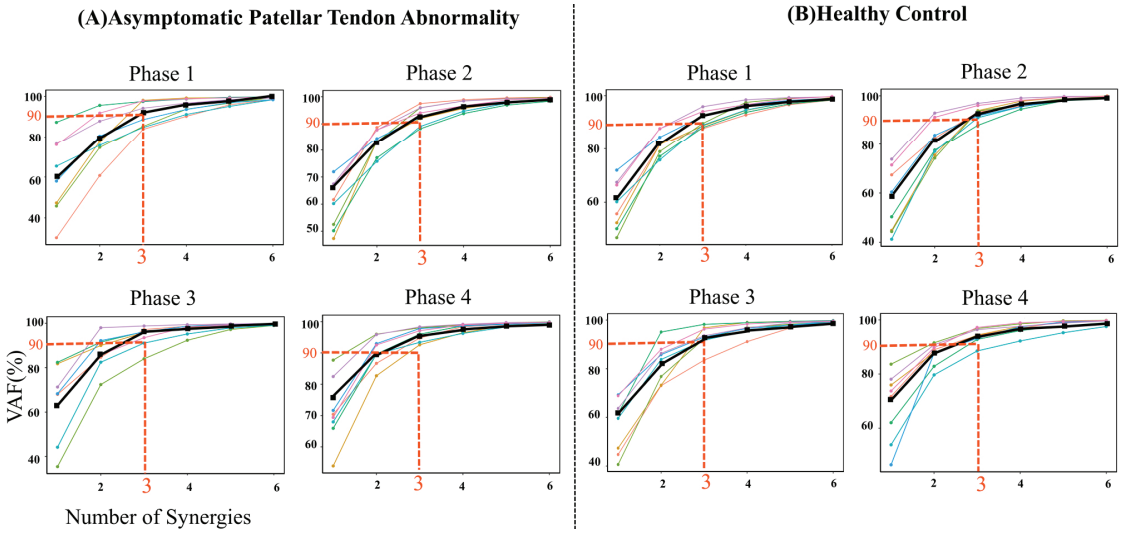

Fig. 2. Individual (thin line) and mean participant (think lines) percentages of the variability accounted for (VAF). (A) and (B) panels show the VAFs of the APTA and the healthy group, respectively. The horizontal dashed lines indicate the thresholds used to determine the number of extracted lower limb muscle synergies

92.56%, respectively. The average VAF within all groups exceeded 90%. However, when the number of synergies increased to 4, the average VAF improvement was less than 2%, so the number of synergies was ultimately set at 3 for further analysis.

3.2. Features of muscle synergy extraction

In Figures 3 and 4, the muscle weights and temporal activation patterns during the stop-jump process for the APTA and Healthy groups across the four phases, respectively, are illustrated. In Figure 5, a heatmap of the muscle weights in the lower limbs during the stop-jump across the four phases for the APTA and Healthy groups is provided. Based on the temporal structure, the classification of muscle synergies corresponds to specific movement phases during the stop-jump process, with each cycle consisting of three distinct phases: initial ground contact, braking, and vertical jump phases. Based on the timing of peak occurrence, the waveform of Synergy1 is associated with the initial ground contact phase of the stop-jump, with the peak appear-

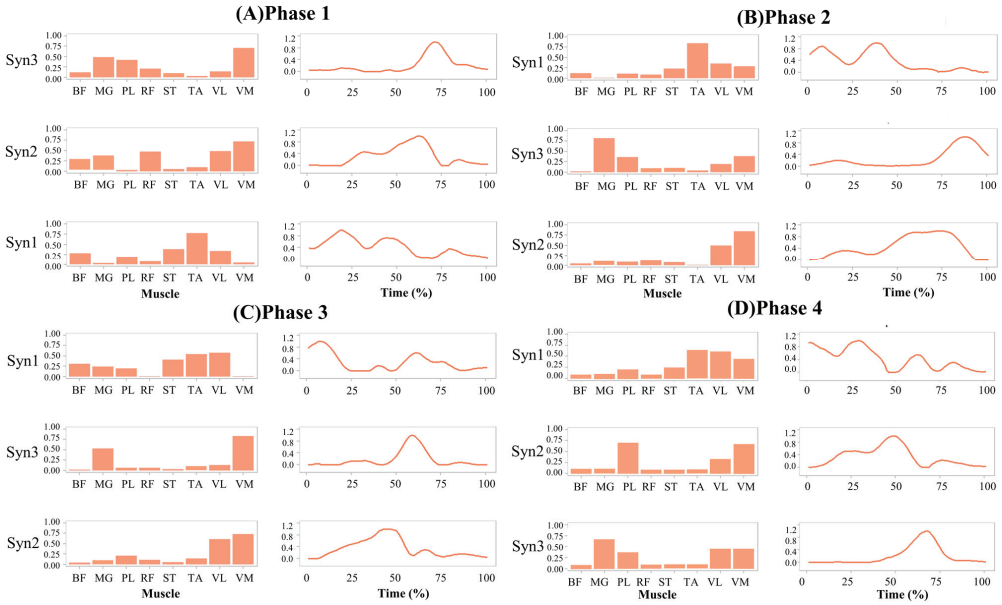

Fig. 3. The muscle synergy extraction for the APTA group. (A), (B), (C), and (D) represent the muscle synergies for P1, P2, P3 and P4, respectively, extracted from 8 leg muscles and used for functional classification during the stop-jump movement. Left – muscle weights; Right – activation patterns; Syn – Synergy

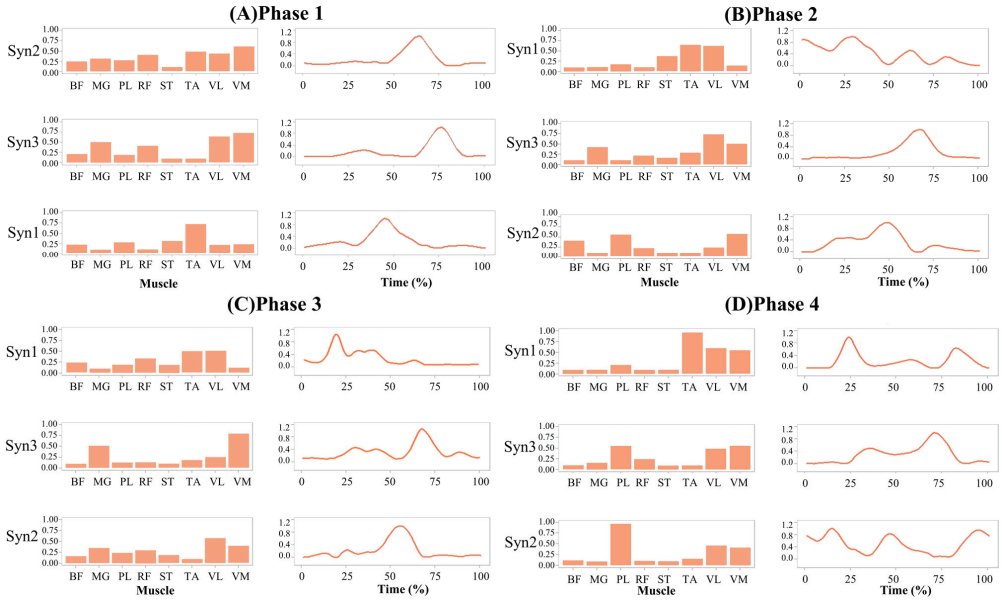

Fig. 4. The muscle synergy extraction for the Healthy group. (A), (B), (C) and (D) represent the muscle synergies for P1, P2, P3 and P4, respectively, extracted from 8 leg muscles and used for functional classification during the stop-jump movement. Left – muscle weights, Right – activation patterns, Syn – Synergy

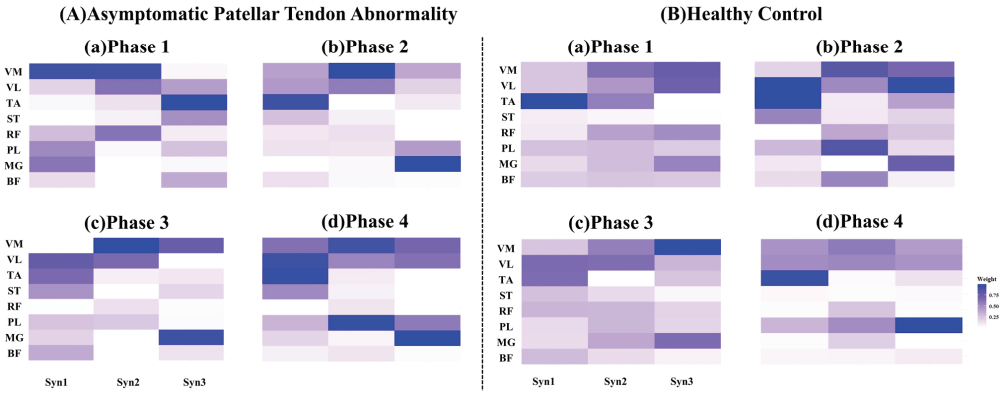

Fig. 5. Heatmap of muscle weights during the 4 phases of the stop-jump for the APTA and the healthy group. Syn – Synergy

ing at the start of the action (0–30%) and then declining. The waveform of Synergy1 is mainly influenced by the weights of TA, ST, and VL. The main peak of Synergy2 appears in the braking phase (30–60%), with activation increasing during this phase and then decreasing. The waveform of Synergy2 is mainly determined by the weights of BF, ST, VL, VM and MG. The waveform of Synergy3 appears during the vertical jump phase (60–100%), and is mainly determined by the weights of VL, VM, RF, PL and MG.

3.3. APTA and Healthy group differences in each synergy across four loading phases

In Figure 6, a detailed overview of the muscle weight comparison between the APTA and Healthy groups across the four phases in the three synergies is provided. In Synergy 1, the interaction between groups and load accumulation for VM has statistical significance, $F(3, 21) = 2.669$, $p = 0.041$, $\eta^2 = 0.16$. The interaction between groups and load accumulation for ST is statistically significant, $F(3, 21) = 3.022$, $p = 0.038$, $\eta^2 = 0.19$. Specifically, the VM weight in the APTA group was significantly higher than that in the Healthy group during the P1 and P2, with differences of 0.45 and 0.25, respectively ($p < 0.05$). Meanwhile, in the P3 and P4, the ST weight in the APTA group was significantly higher than that in the Healthy group, with differences of 0.18 and 0.30, respectively ($p < 0.05$).

In Synergy 2, the interaction between groups and load accumulation for MG is statistically significant, $F(3, 21) = 3.135$, $p = 0.035$, $\eta^2 = 0.19$. The interaction between groups and load accumulation for BF is statis-

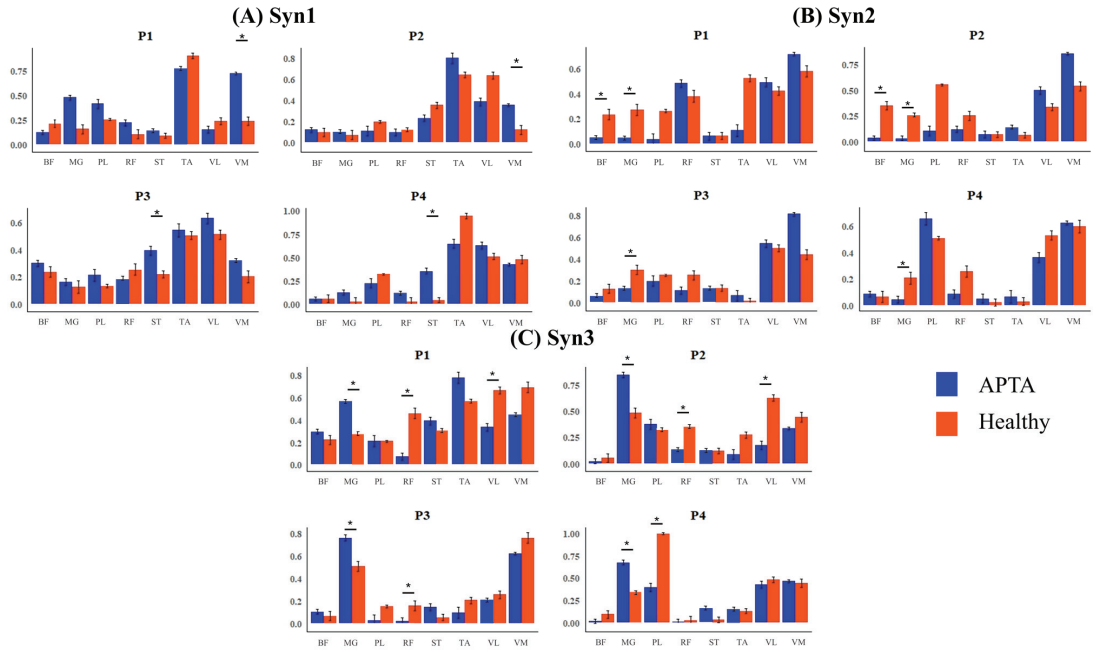

Fig. 6. Diagram of the differences in muscle weights across three synergies during different phases for the APTA and the Healthy group. Syn – Synergy

tically significant, $F(3, 21) = 5.266$, $p = 0.021$, $\eta^2 = 0.26$. Specifically, the MG muscle weight in the Healthy group was significantly higher than in the APTA group at all phases, with differences of 0.18, 0.17, 0.14, and 0.12, respectively ($p < 0.05$). Additionally, the BF weight in the Healthy group was significantly higher than in the APTA group during the P1 and P2 phases, with differences of 0.18 and 0.25, respectively ($p < 0.05$).

In Synergy 3, the interaction between groups and load accumulation for MG is statistically significant, $F(3, 21) = 6.031$, $p = 0.005$, $\eta^2 = 0.43$. The interaction between groups and load accumulation for RF is statistically significant, $F(3, 21) = 5.771$, $p = 0.009$, $\eta^2 = 0.36$. The interaction between groups and load accumulation for VL is statistically significant, $F(3, 21) = 5.012$, $p = 0.017$, $\eta^2 = 0.25$. Specifically, the MG weight in the APTA group was significantly higher than in the Healthy group at all four phases, with differences of 0.33, 0.31, 0.28 and 0.43 ($p < 0.05$), while the Healthy group showed significant advantages in RF and VL at multiple phases. Specifically, the RF weight in the Healthy group was significantly higher than in the APTA group during the P1, P2 and P3 phases, with differences of 0.35, 0.21, and 0.12, respectively ($p < 0.05$). The VL weight in the Healthy group was also significantly higher than in the APTA group during the P1 and P2 phases, with differences of 0.35 and 0.47, respectively ($p < 0.05$).

3.4. The trend of lower limb muscle weight in the APTA and the Healthy group across four phases

In Figure 7, the trends in lower limb muscle weights across the four phases in the APTA and Healthy groups under the three synergies are shown. In Synergy 1, the relative weight of the ST in the APTA group was low in P1 but significantly increased in phases P2 and P3 ($p < 0.05$). The TA had a higher weight in P1 but significantly decreased in phases P2 and P3 ($p < 0.05$). The VL exhibited low activity in P1, which significantly increased in P2 and P3 ($p < 0.05$). The muscle activity in the Healthy group was relatively stable across all four phases. In Synergy 2, the VM and MG in the APTA group showed low activity in P1, but significantly increased in P2 and P3 ($p < 0.05$). The BF in the APTA group had higher activity in P1, then gradually decreased ($p < 0.05$). The PL exhibited higher activity in P1, followed by a significant decrease in P2 and P3 ($p < 0.05$). The BF in the Healthy group had low activity in P1 and P2, but significantly increased in P3 and P4 ($p < 0.05$). The activity of other muscles remained relatively stable. In Synergy 3, the MG, RF, and ST in the APTA group had low activity in P1 but significantly increased in P2 and P3 ($p < 0.05$), while the PL had high activity in P1 but significantly decreased in P2 and P3 ($p < 0.05$). The muscle activity in the Healthy group remained stable across all four phases.

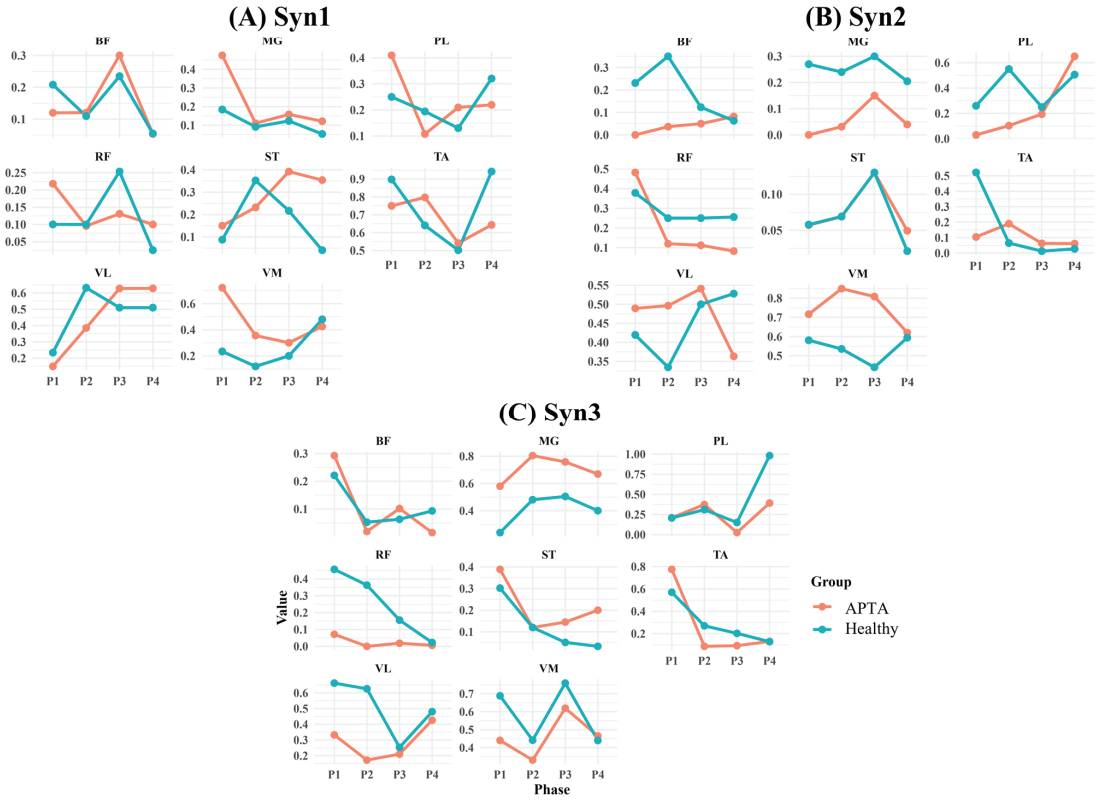

Fig. 7. The activity trend chart of the APTA and the Healthy group in three synergies across four phases. Syn – Synergy

4. Discussion

This study aimed to investigate the muscle synergy patterns in the APTA individuals during the stop-jump task. To our knowledge, this study is the first to quantitatively detail the modular organization strategy of neuromotor responses in APTA individuals during stop-jump. This study reveals the following key findings: (1) APTA individuals exhibit higher ST activity during the landing phase of stop-jump, emphasizing its critical role in the central nervous system's modular control strategy. (2) During the braking phase, APTA individuals exhibit deficiencies in the coordination of multi-muscle control, particularly in the altered spatial and temporal patterns of muscle synergies involving the BF and MG. (3) During the vertical jump phase, APTA individuals display an abnormal muscle synergy pattern with higher MG activity contribution and lower VM and VL contributions, which may be an adaptive response. The results support our hypothesis that there is no significant difference in the number of muscle synergies between the two groups; APTA individuals may adapt to biomechanical changes induced by their condition by adjusting the activity weights of different muscles within each motor module.

In our analysis, we included 8 lower limb muscles because we focused on the synergies between muscles during the stop-jump. We analyzed the four phases of load accumulation in both APTA and Healthy individuals to effectively reveal motor control deficits in the APTA individuals [2], [11], [14]. However, our findings indicate that there is no significant difference in the VAF of the three extracted synergies between the groups. Overall, the muscle synergies and their temporal patterns were strikingly similar between the two groups. This aligns with previous research on APTA individuals during the stop-jump task, indicating that despite variations in motor performance, APTA individuals mobilize similar muscle synergies through compensatory mechanisms to effectively execute the stop-jump task [38]. This also supports the existing view that neuromuscular adaptations do not necessarily alter the overall structure of motor modules, but rather modify the activation patterns within existing modules [7]. This provides a new perspective, revealing that despite underlying pathologies, muscle synergies remain relatively stable. This finding is of significant importance for rehabilitation strategies aimed at maintaining neuromuscular function. Even in the presence of underlying tendon abnormalities, the neuromuscular system may maintain a similar motor pattern

through adaptive adjustments, which could explain the lack of significant differences in synergy patterns.

At a functional level, the muscle synergies obtained in this study correspond to the previously described biomechanical characteristics of stop-jump. A complete stop-jump cycle includes the initial ground contact phase, the braking phase, and the vertical take-off phase. In the initial ground contact phase (0–30%), the primary muscles involved are the TA, ST, and VL, with TA activity initiating at ground contact (as indicated in Fig. 3A's syn1), likely to stabilize the ankle during early dorsiflexion [13]. With load accumulation, the TA's weight contribution diminishes in P3 (Fig. 7A), possibly causing ankle instability and reducing the ankle's ability to absorb ground impact due to decreased TA eccentric contraction, thus increasing knee stress and the risk of knee injury [9]. Therefore, APTA individuals need to strengthen the power and endurance of ankle flexors and enhance eccentric contraction muscles like ST to better control knee flexion. In the P1 and P2, there is a difference in the VM weight contribution to Syn1 between the APTA and Healthy groups (Fig. 6A). During initial ground contact, the VM weight contribution in the APTA group is higher than in the Healthy group, indicating a compensatory mechanism, possibly through increased VM activation to stabilize the knee and prevent excessive flexion or instability. The eccentric contraction of VM helps absorb impact and slow down knee flexion, thereby reducing stress on the patellar tendon [41]. With load accumulation, ST's weight contribution peaks in P3 (Fig. 7A). As a knee flexor, ST is closely related to knee flexion during the stop-jump. During the landing phase, the eccentric contraction of ST helps absorb ground reaction forces, reducing knee impact [29].This study uses NMF to further emphasize the importance of TA, ST and VM in neuromotor control among APTA individuals and reveals a clinical phenomenon: APTA individuals adapt to increased loads by enhancing the strength and stability of ankle muscles and strengthening knee flexors to absorb more impact.

Dorsiflexion during the braking phase (30–60%) is accompanied by subsequent knee flexion. In the recorded muscle activity of this study, BF, ST, VL, VM and MG are responsible for knee flexion, explaining the additional activity of BF and MG in synergy1. We observed deficits in multi-muscle coordination control during the braking phase in the APTA individuals, as evidenced by changes in the spatial and temporal patterns of BF and MG muscle synergies. In Figure 6B, it is shown that the MG activation weight in the APTA group was significantly lower than that in the Healthy group across all four phases, with BF activation also notably lower in P1, P2 and P4. This supports earlier findings that the APTA group tends to rely on other muscles by adjusting motor module functions, resulting in reduced BF and MG activation [39]. Previous studies have found that pain-avoidance strategies and long-term joint abnormalities affect muscle activation patterns [18]. Although APTA individuals do not exhibit obvious pain symptoms, chronic patellar tendon abnormalities may subconsciously lead them to adopt pain-avoidance strategies to reduce pressure on the patellar tendon. This strategy might reduce their reliance on muscles associated with the patellar tendon region (e.g., BF and MG) during the landing cushioning phase, thereby lessening the tensile and shear forces on the patellar tendon. Individuals with musculoskeletal abnormalities adapt neuromuscular control by redistributing muscle activity to reduce the load on the affected tendons [23]. This finding further confirms that the CNS adjusts motor control strategies to protect vulnerable areas, thereby reducing the risk of injury aggravation. As load accumulates, the activation weight of VM and MG increases, while the activation weight of BF and PL decreases, as shown in Fig. 7B. Thus, APTA individuals might enhance knee control by increasing VM and MG activation to prevent excessive knee flexion, thereby reducing patellar tendon load. Previous studies have shown that people with patellar tendinopathy use protective strategies under fatigue to avoid additional stress on the patellar tendon, including proximal compensation and stiff lower limb landing[40], which aligns with the conclusions of this study. PL helps counter the inversion stress generated during landing in the stop-jump, aiding in resisting varus or valgus torques at the knee and further ensuring joint stability. This phenomenon is observed not only in Synergy2 but also in Synergy3. Consequently, APTA individuals face an increased risk of injury during load accumulation. Therefore, APTA individuals are advised to strengthen VM and MG through power training, while also enhancing BF and PL endurance [3].

The vertical take-off phase (60–100%) typically involves the activation of the hip extensors, knee extensors and ankle flexors [24]. In the initial phase of the ascent, VM and VL contribute most of the concentric movement, while the contribution of the gastrocnemius gradually increases in the later phase [12]. However, we noticed that in the early ascent phase, the APTA group displayed an abnormal muscle synergy pattern, with higher MG activity and relatively lower contributions from VM and VL (Fig. 6C). In actual competition, pressure, tension and the game outcome can all affect neuromuscular control. However, the simulated game environment lacks these psychologi-

cal factors, which may lead to insufficient muscle activation in athletes. Previous studies have shown that insufficient quadriceps activation can lead to inadequate knee extension [16]. We also found that the effect size of the interaction between group and load accumulation for MG reached 0.43, indicating that as the load changes, APTA individuals may adapt their knee joint load by adjusting MG activation to reduce the burden on the knee joint, thereby lowering the risk of injury. Consequently, APTA individuals may compensate for insufficient knee extension by increasing gastrocnemius activation, providing more force during the initial phase of the jump. The recruitment sequence and relative contribution from hip extensors to knee extensors and finally to ankle flexors can also be observed in similar movements, such as reverse jumping or transitioning from sitting to standing. This might indicate that stable motor patterns naturally develop after mastering complex lower limb movements.

When discussing muscle synergy, the number of muscles chosen and the number of synergies selected significantly influence the results. In this study, we focused only on the 8 lower limb muscles, as the research emphasized the synergy between these muscles during the stop-jump process. However, future research should further explore the contribution of upper limb muscles (e.g., latissimus dorsi) and trunk muscles (e.g., erector spinae, rectus abdominis and external oblique) to assess the relationship between upper and lower limb muscle synergy in complex movements. Moreover, this study was carried out in a laboratory environment, with strictly controlled conditions, but it could not entirely simulate the complexities of a real basketball game. Therefore, future research should consider being conducted on an actual basketball court to observe athletes' muscle synergies during real game situations. Another limitation of this study is its short duration, making it difficult to determine whether motor module control causes injuries or if injuries lead to changes in motor module control. Future research should involve long-term prospective studies to further investigate this causal relationship. Additionally, the use of dimensionality reduction techniques is also a topic of debate. Some researchers argue that specific muscle synergies reflect motor commands specifically adjusted by the central nervous system for particular tasks, while others suggest that these synergies might simply be artifacts of the decomposition algorithm used [5]. Regardless of the viewpoint, further research is needed to explore the underlying mechanisms of these muscle synergies. Future research should broaden its scope to cover more motor tasks, providing a more comprehensive understanding of motor module control in the APTA individuals.

5. Conclusions

The main purpose of this study was to investigate the muscle synergy patterns of the APTA individuals during the stop-jump. The results showed that although there were no significant differences in the number of muscle synergies and the VAF of the extracted synergy patterns between the APTA and healthy groups, the APTA group exhibited significantly abnormal muscle synergy patterns in specific phases and under load accumulation conditions. These abnormalities mainly occurred in the ST, MG, BF, and PL, suggesting that APTA individuals might use compensatory mechanisms to avoid excessive load on the patellar tendon. However, this compensatory strategy may increase the risk of injury to the knee joints. Therefore, training for APTA individuals should focus on strengthening the ST and MG muscles and improving the endurance of the BF and PL muscles to enhance joint stability and prevent patellar tendinopathy.

Funding

This study was sponsored by Zhejiang Province Key R&D program of "Pioneer" and "Leader" (2023C03197), Zhejiang Province Science Fund for Distinguished Young Scholars (Grant number: LR22A020002), Ningbo Key Research and Development Program (Grant number: 2022Z196), Zhejiang Rehabilitation Medical Association Scientific Research Special Fund (ZKKY2023001), Research Academy of Medicine Combining Sports, Ningbo (No. 2023001), the Project of Ningbo Leading Medical & Health Discipline (No. 2022-F15, No. 2022-F22), Ningbo Natural Science Foundation (Grant number: 2022J065) and K. C. Wong Magna Fund in Ningbo University.

References

[1] BARRADAS V.R., KUTCH J.J., KAWASE T., KOIKE Y., SCHWEIGHOFER N., *When 90% of the variance is not enough: residual EMG from muscle synergy extraction influences task performance*, J. Neurophysiol., 2020, 123 (6), 2180–2190.

[2] BENÍTEZ-MARTÍNEZ J.C., VALERA-GARRIDO F., MARTÍNEZ--RAMÍREZ P., RÍOS-DÍAZ J., DEL BAÑO-ALEDO M.E., MEDINA-MIRAPEIX F., *Lower Limb Dominance, Morphology, and Sonographic Abnormalities of the Patellar Tendon in Elite Basketball Players: A Cross-Sectional Study*, J. Athl. Train., 2019, 54 (12), 1280–1286.

[3] CHALLOUMAS D., PEDRET C., BIDDLE M., NG N.Y.B., KIRWAN P., COOPER B. et al., *Management of patellar tendinopathy: a systematic review and network meta-analysis of randomised studies*, BMJ Open Sport Exerc. Med., 2021, 7 (4), e001110.

[4] COOK J.L., KHAN K.M., KISS Z.S., COLEMAN B.D., GRIFFITHS L., *Asymptomatic hypoechoic regions on patellar tendon ultrasound: A 4-year clinical and ultrasound followup of 46 tendons*, Scand. J. Med. Sci. Sports, 2001, 11 (6), 321–327.

[5] COSCIA M., CHEUNG V.C., TROPEA P., KOENIG A., MONACO V., BENNIS C. et al., *The effect of arm weight support on upper limb muscle synergies during reaching movements*, J. Neuroeng. Rehabil., 2014, 11, 22.

[6] D'AVELLA A., *Modularity for Motor Control and Motor Learning*, Adv. Exp. Med. Biol., 2016, 957, 3–19.

[7] D'AVELLA A., GIESE M., IVANENKO Y.P., SCHACK T., FLASH T., *Editorial: Modularity in motor control: from muscle synergies to cognitive action representation*, Front Comput. Neurosci., 2015, 9,126.

[8] DAL PUPO J., DETANICO D., ACHE-DIAS J., SANTOS S.G., *The fatigue effect of a simulated futsal match protocol on sprint performance and kinematics of the lower limbs*, J. Sports Sci., 2017, 35 (1), 81–88.

[9] DURY J., MICHEL F., RAVIER G., *Fatigue of hip abductor muscles implies neuromuscular and kinematic adaptations of the ankle during dynamic balance*, Scand. J. Med. Sci. Sports, 2022, 32 (9), 1324–1334.

[10] EDWARDS S., STEELE J.R., MCGHEE D.E., BEATTIE S., PURDAM C., COOK J.L., *Landing strategies of athletes with an asymptomatic patellar tendon abnormality*, Med. Sci. Sports Exerc., 2010, 42 (11), 2072–2080.

[11] EDWARDS S., STEELE J.R., MCGHEE D.E., PURDAM C.R., COOK J.L., *Asymptomatic players with a patellar tendon abnormality do not adapt their landing mechanics when fatigued*, J. Sports Sci., 2017, 35 (8), 769–776.

[12] ESCAMILLA R.F., *Knee biomechanics of the dynamic squat exercise*, Med. Sci. Sports Exerc., 2001, 33 (1), 127–141.

[13] ALVES F.S.M., OLIVEIRA F.S., JUNQUEIRA C., AZEVEDO B.M.S., DIONÍSIO V.C. (eds.), *Analysis of electromyographic patterns during standard and declined squats*, Brazilian Journal of Physical Therapy, 2009.

[14] HARRIS M., SCHULTZ A., DREW M.K., RIO E., ADAMS S., EDWARDS S., *Thirty-seven jump-landing biomechanical variables are associated with asymptomatic patellar tendon abnormality and patellar tendinopathy: A systematic review*, Phys. Ther. Sport., 2020, 45, 38–55.

[15] HARRIS M., SCHULTZ A., DREW M.K., RIO E., CHARLTON P., EDWARDS S., *Jump-landing mechanics in patellar tendinopathy in elite youth basketballers*, Scand. J. Med. Sci. Sports, 2020, 30 (3), 540–548.

[16] HART J.M., PIETROSIMONE B., HERTEL J., INGERSOLL C.D., *Quadriceps activation following knee injuries: a systematic review*, J. Athl. Train., 2010, 45 (1), 87–97.

[17] HERMENS H.J., FRERIKS B., DISSELHORST-KLUG C., RAU G., *Development of recommendations for SEMG sensors and sensor placement procedures*, J. Electromyogr. Kinesiol., 2000, 10 (5), 361–374.

[18] HODGES P.W., TUCKER K., *Moving differently in pain: a new theory to explain the adaptation to pain*, Pain, 2011, 152 (3 Suppl.), S90–s8.

[19] HUTCHISON M.K., HOUCK J., CUDDEFORD T., DOROCIAK R., BRUMITT J., *Prevalence of Patellar Tendinopathy and Patellar Tendon Abnormality in Male Collegiate Basketball Players: A Cross-Sectional Study*, J. Athl. Train., 2019, 54 (9), 953–958.

[20] JIE T., XU D., ZHANG Z., TEO E.C., BAKER J.S., ZHOU H. et al., *Structural and Organizational Strategies of Locomotor Modules during Landing in Patients with Chronic Ankle Instability*, Bioengineering, Basel, 2024, 11 (5).

[21] JILDEH T.R., BUCKLEY P., ABBAS M.J., PAGE B., YOUNG J., MEHRAN N. et al., *Impact of Patellar Tendinopathy on Player Performance in the National Basketball Association*, Orthop. J. Sports Med., 2021, 9 (9), 23259671211025305.

[22] KERKMAN J.N., DAFFERTSHOFER A., GOLLO L.L., BREAKSPEAR M., BOONSTRA T.W., *Network structure of the human musculoskeletal system shapes neural interactions on multiple time scales*, Sci. Adv., 2018, 4 (6), eaat0497.

[23] KHOU S.B., SAKI F., TAHAYORI B., *Muscle activation in the lower limb muscles in individuals with dynamic knee valgus during single-leg and overhead squats: a meta-analysis study*, BMC Musculoskeletal. Disorders, 2024, 25 (1), 652.

[24] KUBO K., IKEBUKURO T., YATA H., *Effects of squat training with different depths on lower limb muscle volumes*, Eur. J. Appl. Physiol., 2019, 119 (9), 1933–1942.

[25] LATASH M.L., *Motor synergies and the equilibrium-point hypothesis*, Motor Control., 2010, 14 (3), 294–322.

[26] LEE D.D., SEUNG H.S., *Algorithms for non-negative matrix factorization*, Proceedings of the 13th International Conference on Neural Information Processing Systems; Denver, CO, MIT Press, 2000. 535–541.

[27] LI F., SONG Y., CEN X., SUN D., LU Z., BÍRÓ I. et al., *Comparative Efficacy of Vibration foam Rolling and Cold Water Immersion in Amateur Basketball Players after a Simulated Load of Basketball Game*, Healthcare (Basel), 2023, 11 (15).

[28] MA Y., SHI C., XU J., YE S., ZHOU H., ZUO G., *A Novel Muscle Synergy Extraction Method Used for Motor Function Evaluation of Stroke Patients: A Pilot Study*, Sensors, (Basel), 2021, 21 (11).

[29] MALLIARAS P., BARTON C.J., REEVES N.D., LANGBERG H., *Achilles and patellar tendinopathy loading programmes: a systematic review comparing clinical outcomes and identifying potential mechanisms for effectiveness*, Sports Med., 2013, 43 (4), 267–286.

[30] PIETROSIMONE L.S., BLACKBURN J.T., WIKSTROM E.A., BERKOFF D.J., DOCKING S.I., COOK J. et al., *Differences in Biomechanical Loading Magnitude During a Landing Task in Male Athletes with and without Patellar Tendinopathy*, J. Athl. Train., 2021, 57 (11–12), 1062–1071.

[31] SAITO H., YOKOYAMA H., SASAKI A., KATO T., NAKAZAWA K., *Evidence for basic units of upper limb muscle synergies underlying a variety of complex human manipulations*, J. Neurophysiol., 2022, 127 (4), 958–968.

[32] SANTUZ A., EKIZOS A., JANSHEN L., MERSMANN F., BOHM S., BALTZOPOULOS V. et al., *Modular Control of Human Movement During Running: An Open Access Data Set*, Front Physiol., 2018, 9, 1509.

[33] SAWERS A., ALLEN J.L., TING L.H., *Long-term training modifies the modular structure and organization of walking balance control*, J. Neurophysiol., 2015, 114 (6), 3359–3373.

[34] SCANLAN A.T., DASCOMBE B.J., REABURN P.R., *The construct and longitudinal validity of the basketball exercise simulation test*, J. Strength Cond. Res., 2012, 26 (2), 523–530.

[35] SHARIF F., AHMAD A., SHABBIR A., *Does the ultrasound imaging predict lower limb tendinopathy in athletes: a systematic review*, BMC Med. Imaging, 2023, 23 (1), 217.

[36] TAYFUR A., HAQUE A., SALLES J.I., MALLIARAS P., SCREEN H., MORRISSEY D., *Are Landing Patterns in Jumping Athletes Associated with Patellar Tendinopathy? A Systematic Review with Evidence Gap Map and Meta-analysis*, Sports Med., 2022, 52 (1), 123–137.

[37] TIGRINI A., VERDINI F., FIORETTI S., MENGARELLI A., *On the Decoding of Shoulder Joint Intent of Motion From Transient EMG: Feature Evaluation and Classification*, IEEE Transactions on Medical Robotics and Bionics, 2023, 5, 1037–1044.

[38] TODOROV E., *Optimality principles in sensorimotor control*, Nat. Neurosci., 2004, 7 (9), 907–915.

[39] VAN DER WORP H., VAN ARK M., ROERINK S., PEPPING G.J., VAN DEN AKKER-SCHEEK I., ZWERVER J., *Risk factors for patellar tendinopathy: a systematic review of the literature*, Br. J. Sports Med., 2011, 45 (5), 446–452.

[40] VERMEULEN S., DE BLEECKER C., SPANHOVE V., SEGERS V., WILLEMS T., ROOSEN P. et al., *The effect of fatigue on spike jump biomechanics in view of patellar tendon loading in volleyball*, Scand. J. Med. Sci. Sports, 2023, 33 (11), 2208–2218.

[41] VINCENT K.R., VASILOPOULOS T., MONTERO C., VINCENT H.K., *Eccentric and Concentric Resistance Exercise Comparison for Knee Osteoarthritis*, Med. Sci. Sports Exerc., 2019, 51 (10), 1977–1986.

[42] WANG Y.-X., ZHANG Y., *Nonnegative Matrix Factorization: A Comprehensive Review*, IEEE Transactions on Knowledge and Data Engineering, 2013, 25, 1336–1353.

[43] YOKOYAMA H., KATO T., KANEKO N., KOBAYASHI H., HOSHINO M., KOKUBUN T. et al., *Basic locomotor muscle synergies used in land walking are finely tuned during underwater walking*, Sci. Rep., 2021, 11 (1), 18480.